ACS ES&T Water

pubs.acs.org/estwater

Article

Rapid Removal of Poly- and Perfluoroalkyl Substances with Quaternized Wood Pulp

Justin T. Harris, Gloria D. de la Garza, Angela M. Devlin, and Anne J. McNeil*

Cite This: ACS EST Water 2022, 2, 349−356

Read Online

ACCESS | Metrics & More | Article Recommendations | Supporting Information

ABSTRACT: Across the United States, many municipalities are utilizing adsorbents to remove pervasive poly- and perfluoroalkyl substances (PFASs) from their drinking water. However, conventional adsorbents usually require long contact times (minutes to days) to achieve high removal efficiencies. To overcome this limitation, we developed materials that rapidly adsorb anionic PFASs from water within seconds. More specifically, we discovered that cellulose fibers functionalized with cationic amines (quaternized wood pulp (QWP)) removed more than 80% of the most prevalent PFASs (perfluorooctanesulfonic acid (PFOS) and perfluorooctanoic acid (PFOA)) within seconds at environmentally relevant concentrations (~2.5 μg/L). In contrast, the QWPs were less efficient at adsorbing shorter chain PFASs (<30%). The maximum adsorption capacity values of the best QWP were found to be 763 and 605 mg/g for PFOS and PFOA, respectively, which are competitive with both conventional and newer adsorbents. This work highlights how functionalized cellulose fibers, which are both bio-sourced and biodegradable, may be a promising material for advancing water treatment technologies.

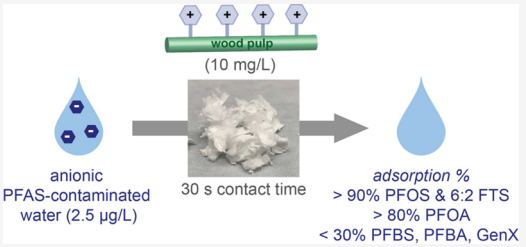

KEYWORDS: *quaternized wood pulp, perfluoroalkyl substances, adsorption, cationic cellulose*

INTRODUCTION

Clean drinking water is increasingly challenging to acquire as many municipalities around the world struggle with pollutants.[1] For example, poly- and perfluoroalkyl substances (PFASs) are found in many fresh water supplies within the United States (US).[2−5] PFASs can be anionic, cationic, nonionic, or zwitterionic; however, anionic PFASs such as perfluorooctanesulfonic acid (PFOS) and perfluorooctanoic acid (PFOA) are most prevalent in the environment.[6,7] PFASs have been employed in aqueous film-forming foam,[7] surfactants,[8] and other consumer goods,[9] but they are being phased out of production[10] because they have been shown to negatively affect biota and human health.[11,12] To limit PFAS pollution, communities around the world are setting guidelines for maximum PFAS concentrations in potable water supplies.[13,14] For example, in 2016, the US Environmental Protection Agency set a health advisory limit of 70 ng/L for the combined PFOS and PFOA levels,[15] and some states are setting even lower limits. For example, Michigan adopted stricter maximum contaminant levels of 16 and 8 ng/L for PFOS and PFOA, respectively, in 2020.[16] Despite these regulations, however, PFASs are still found in potable water sources.[2,17]

Currently, several technologies exist for removing PFASs from water,[18] but adsorption is the most effective strategy. Activated carbon (AC) is the leading adsorbent for PFAS removal because it is inexpensive and exhibits moderate adsorption capacities.[19,20] However, AC has slow adsorption kinetics and long equilibration times (i.e., days).[21,22] Ion exchange (IX) resins are another common adsorbent because they are easy to implement, and they exhibit higher adsorption capacities than AC.[20] Despite these advantages, IX resins also suffer from slow adsorption kinetics and long equilibrium times (i.e., hours to days).[23] These limitations of AC and IX resins demonstrate the need for improved adsorbents with faster adsorption.

Researchers are developing adsorbents to overcome the limitations of AC and IX resins. For example, Leibfarth and co-workers recently reported an ionic fluorogel that uses both fluorophilic and ionic interactions to selectively adsorb PFASs over other organic contaminants (e.g., humic acid). High removal efficiencies (>95%) were observed for most PFASs after 2 h using spiked water samples from a local treatment plant.[24] These ionic fluorogels represent an improvement over the cationic hydrogels reported earlier by Karanfil and co-workers, which demonstrated high removal efficiencies (>80%) after 24 h using spiked water samples from both untreated and treated wastewater.[25] Nevertheless, both hydrogels are derived

Received: October 14, 2021
Revised: December 23, 2021
Accepted: January 12, 2022
Published: January 26, 2022

from non-renewable, petroleum-based feedstocks and will be landfilled at the end of their usable lifetimes.

An alternative, and likely a more sustainable approach, would be to generate adsorbents from renewable resources, specifically ones that can be biodegraded at the end of their usable lifetimes. For example, together, Dichtel and Helbling have developed sustainably sourced cyclodextrin-based adsorbents for pollutant removal.[26,27] In particular, they have shown that cyclodextrins functionalized with amines and permanent cations quickly (contact time = 30 min) adsorb anionic PFASs like PFOS and PFOA at environmentally relevant concentrations.[28−31] Their materials also have shorter equilibration times than AC, and their distribution coefficients (K_D) rival those of AC and IX resins. Cellulose, a biodegradable and renewable biopolymer, is another potential material for generating effective adsorbents,[32] with some researchers already using it to adsorb PFASs.[33,34] For example, Ateia and co-workers showed that poly(ethylenimine)-functionalized cellulose microcrystals (PEI-CMCs) effectively adsorb >90% of several anionic PFASs.[33] In another example, Yu and co-workers demonstrated that cotton grafted with quaternary amines adsorbs ∼70% of PFOS and PFOA and have high adsorption capacities of 1600 and 1300 mg/g, respectively.[34] In both cases, however, the adsorbents required more than 60 min to achieve these efficiencies, demonstrating the need for improved cellulose-based adsorbents with rapid PFAS adsorption.

In previous work, we observed that hydrogels made from anionic sulfated cellulose nanofibers rapidly (<30 s) and efficiently adsorbed (>90%) a cationic dye via electrostatic interactions.[35] We hypothesized that cationic cellulose could be similarly used to rapidly adsorb anionic PFASs via electrostatic interactions. However, cellulose nanofibers are expensive due to their extensive processing; hence, we evaluated an inexpensive alternative, wood pulp (WP). WP is a by-product of the papermaking industry and requires few energy-intensive production steps.[36] Herein, we report that WP functionalized with quaternary amines rapidly (<30 s) and efficiently adsorbs anionic PFASs. Adsorption efficiencies greater than 90 and 80% are achieved at environmentally relevant concentrations for PFOS and PFOA, respectively. Moreover, the adsorption capacities of 763 and 605 mg/g for PFOS and PFOA, respectively, are competitive with other existing adsorbents. Overall, the cationic WP adsorbent is effective for rapidly removing PFASs from spiked water samples at environmentally relevant concentrations.

MATERIALS AND METHODS

QWP Synthesis. Note that throughout the manuscript, quaternized wood pulp (QWP) samples are identified by their charge density (e.g., QWP1.5 is a sample with a charge density of 1.5 mmol $-NR_3^+/g$). The synthesis of QWPs was carried out similar to literature procedures.[37−39] WP (1.0 g) was combined with Millipore water (50 mL) in a 100 mL round-bottom flask. The mixture was left alone for 15 min to wet the fibers, and then the mixture was homogenized at 18K rpm for 2 min. The fibers were soaked for 5 min while the homogenizer was disassembled and cleaned with water and acetone to remove any clogged fibers and then reassembled. The mixture was homogenized again at 18K rpm for 2 min.

The mixture was divided into two 50 mL polypropylene centrifuge tubes and water was added to fill the tubes (∼45 mL in each tube). The tubes were centrifuged at 2580 × g for 4 min, and the supernatant was discarded. The WP from each tube was combined into a round-bottom flask (note: a 100 mL round-bottom flask was used when making QWP1.5 and QWP0.65, but a 250 mL round-bottom flask was used when making QWP0.99, QWP0.97, and QWP0.0). 2-Propanol (50.0 mL) was added to the flask along with NaOH (333.4 mg, 8.335 mmol) and a stir bar. The flask was then heated to 50 °C on a heating block and stirred for 45 min. After this activation time, a known volume of glycidyl trimethyl ammonium chloride (Table S1) was added using a micropipette over 0−4 min to the reaction, and the mixture was stirred for 2.25 h. After the reaction time, the round-bottom flask was removed from the heating block and cooled in ice-cold water for 5 min. The reaction was quenched with 5 M HCl (∼3 mL) and stirred for 5 min. The mixture was vacuum filtered using a VWR grade 413 filter paper and rinsed with Millipore water (1 × 50 mL).

The fibers were then divided into two 50 mL polypropylene centrifuge tubes. Millipore water was added to fill the tubes (∼45 mL in each tube), the tubes were centrifuged at 3260 × g for 7−10 min, and then the supernatant was discarded. This process was defined as one centrifuge cycle, and this centrifuge cycling was repeated two more times to remove excess acid and ions from the fibers. After the third cycle (second cycle for QWP0.0), the pH of the supernatant was examined using a pH paper and found to be ∼7. In addition, the supernatant from one of the tubes was vacuum-filtered, and the conductivity of the supernatant was measured. If the conductivity was ≤25 μS/cm, the fiber purification was considered done. If the conductivity was >25 μS/cm, the centrifuge cycling was repeated until the supernatant could be filtered and measured to have a conductivity ≤25 μS/cm. See Table S1 for the number of centrifuge cycles used to purify each QWP sample. After the fibers were purified, the fibers were removed from the centrifuge tubes with a spatula, placed in 20 mL vials, frozen in liquid N_2, and dried under vacuum to remove excess water.

General Procedure for Adsorbing PFASs. A known volume of PFAS solution was placed in a 50 mL polypropylene centrifuge tube, and in some experiments, a known volume of solution with measured pH, humic acid, or NaCl was added as well. Next, a volume of the QWP mixture with known concentration and a volume of water were syringed over 10 s into the bottom of the centrifuge tube while vortex mixing at a speed of 1.5. The tube was vortex mixed for an additional 10 s using the same speed. The centrifuge tube was removed from the vortex mixer, and an aliquot was taken with a 3 mL plastic syringe, filtered through a cellulose acetate syringe filter, and placed in either a 2 mL glass vial for in-house analysis or a 15 mL centrifuge tube so the sample could be sent to Eurofins Eaton Analytical for analysis (see the Supporting Information).

RESULTS AND DISCUSSION

Quaternized Wood Pulp Synthesis and Characterization. To test our hypothesis that cationic cellulose could rapidly adsorb PFASs via electrostatic interactions, several different QWPs were synthesized by varying the relative concentration of glycidyl trimethyl ammonium chloride (GMAC) to obtain charge densities ranging from 0.0−1.5 mmol $-NR_3^+/g$ (Scheme 1).[37−39] Conductometric titrations were performed to determine charge densities (Table S2), and elemental analysis was used to verify the titration results (Table S3).[40] Previous work by Westman and de la Motte, wherein cellulose was reacted with GMAC, suggests that

https://doi.org/10.1021/acsestwater.1c00396
ACS EST Water 2022, 2, 349−356

Scheme 1. QWP Fiber Synthesis with Various Charge Densities

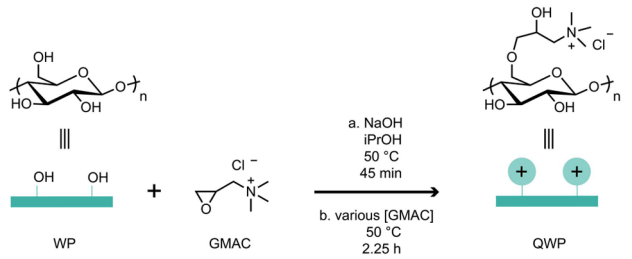

quaternary amines are primarily located at the C2 and C6 positions on the glucose repeat unit.[40] An infrared spectrum acquired on QWP1.5 showed a band at 1480 cm^{-1} that is not present in unfunctionalized QWP0.0, consistent with the added methyl ammonium moiety (Figure S8).[41]

These cationic wood pulp fibers are likely more hydrophilic than the unfunctionalized wood pulp based on contact angle measurements on similarly functionalized cellulose materials.[42] Scanning electron microscopy images were collected on both unfunctionalized and functionalized WP fibers, showing negligible changes in fiber dimensions during synthesis (Figure S7). Auger electron spectroscopic analysis of the surfaces provided support for the intended N functionalization. Because these WP fibers have both surface and interior (amorphous) sites that can be functionalized,[38,43,44] Raman spectroscopy was performed on the fiber surface, at different depths, and throughout a cross-section to determine where functionalization occurred. More specifically, we used the quaternary amine's symmetric stretch at 764 cm^{-1} to map the functional group location. The Raman spectra acquired on a cross-section showed similarly intense symmetric stretches at all locations (Figures 1B and Figure S2),[45] while lateral and depth maps

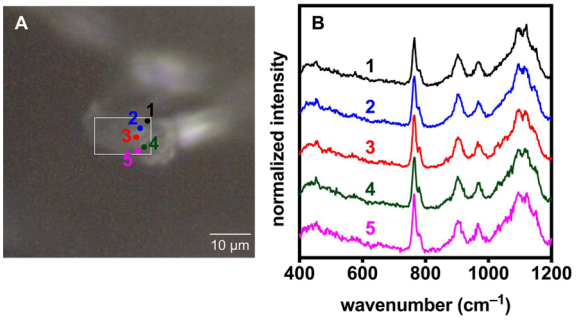

Figure 1. (A) Microscope image of a QWP1.5 fiber cross-section. (B) Raman spectra acquired at various positions on the fiber's cross-section. (The Raman spectra were normalized to the peak at 1096 cm^{-1}, which corresponds to the C−O and C−C stretches.)

also showed similar intensities (Figures S3 and S4). As a control, the unfunctionalized QWP0.0 was also mapped, showing the expected absence of any peaks at 764 cm^{-1} (Figures S3, S5, and S6). Overall, these results indicate that amination occurs throughout QWP fibers and are not preferentially located on the surface.

PFOS and PFOA Adsorption Efficiencies. After synthesizing QWPs with a range of charge densities (CDs), we next examined their PFAS adsorption efficiencies, anticipating that the wood pulp with the highest charge density would exhibit the highest removal efficiency based on electrostatic interactions. To test this hypothesis, QWPs with CDs from 0.0 to 1.5 mmol $-NR_3^+/g$ were mixed in PFOS or PFOA solutions, and adsorption was analyzed after 30 s of contact time (Figure 2A). As expected, nearly 100% of PFOS

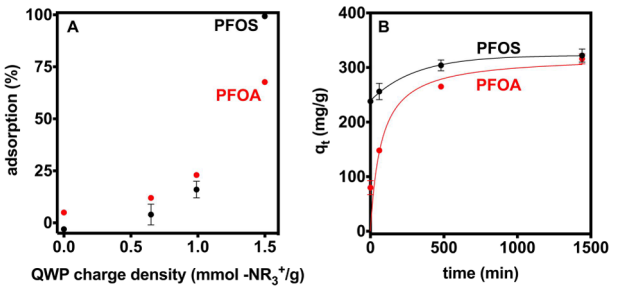

Figure 2. (A) Effect of QWP charge density on PFOS (black) and PFOA (red) adsorption percents. ([QWP] = 50.0 mg/L, $[PFOS]_0$ = 4.2 mg/L, and $[PFOA]_0$ = 3.9 mg/L.) (B) PFOS (black) and PFOA (red) adsorption capacities (q_t) over time on QWP1.5. ([QWP1.5] = 10.0 mg/L, $[PFOS]_0$ = 3.5 mg/L, and $[PFOA]_0$ = 3.9 mg/L.) Note that the first time point is at 30 s. Some error bars are not visible due to their small size.

and 70% of PFOA were removed from solution with the highest CD QWP (QWP1.5), while QWPs with lower CDs (QWP0.99 and QWP0.65) adsorbed less than 16% of PFOS and 23% of PFOA. These results demonstrate that higher wood pulp CDs lead to more PFOS/PFOA adsorption under otherwise identical conditions. Moreover, because the unfunctionalized WP (i.e., with no cationic charges) removed a negligible amount of anionic PFAS, we concluded that the PFAS adsorption on QWPs likely occurs via electrostatic interactions. Moving forward, QWP1.5 was used for the remainder of the studies because it exhibited the highest adsorption percent compared to the other QWPs.

To optimize adsorption capacity, we added varying amounts of QWP1.5 to PFOS solutions and measured PFOS adsorption after 30 s of contact time (Figure S16). A small QWP1.5 dosage of 1.25 mg/L resulted in negligible PFOS adsorption, but increasing the dosage to 12.5 mg/L resulted in a PFOS adsorption capacity of 263 ± 3 mg/g. Further increasing the dosage to 50.0 mg/L resulted in a decreased adsorption capacity of approximately 80 mg/g. This trend suggests that employing too much QWP1.5 results in inefficient use of available cationic sites, and a moderate dosage maximizes PFAS adsorption. Thus, we utilized a dosage of 10.0 mg/L for the remaining studies.

Equilibrium Adsorption Capacities. To determine if adsorption equilibrium is achieved within 30 s of contact time, PFOS and PFOA adsorption capacities (q_t) on QWP1.5 were monitored over 24 h (Figure 2B). After 30 s of contact time, the PFOS adsorption capacity was 238 ± 5 mg/g, corresponding to 67 ± 1% of PFOS adsorbed, while PFOA adsorption capacity was 80 ± 10 mg/g, with 20 ± 3% of PFOA adsorbed. The adsorption equilibrium required 8 and 24 h of contact time for PFOS and PFOA, respectively, suggesting that longer times are needed to reach higher adsorption capacities.

Adsorption isotherms were generated to determine the QWP1.5's maximum adsorption capacities for PFOS and PFOA. Isotherm data were collected by soaking QWP1.5 in either PFOS or PFOA solutions for 24 h and measuring the equilibrium PFOS/PFOA concentrations (C_e) in solution (Figure 3 and Tables S12 and S13). The resulting data were fit

https://doi.org/10.1021/acsestwater.1c00396
ACS EST Water 2022, 2, 349−356

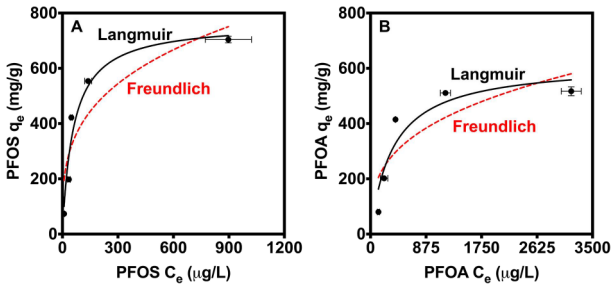

Figure 3. Plots of equilibrium adsorption capacities (q_e) versus equilibrium concentrations (C_e) for (A) PFOS and (B) PFOA, fit with the Langmuir (solid black line) and Freundlich (dashed red line) models. ([QWP1.5] = 10.0 mg/L, $[PFOA]_0$ = ~920−8300 μg/L, and $[PFOS]_0$ = ~750−8000 μg/L. Some error bars are not visible due to their small size.)

with Langmuir and Freundlich isotherm models. The Langmuir model was found to best fit the data, according to a linear least-squares regression (Tables S14 and S15). Because the Langmuir model best describes the equilibrium adsorption behavior, adsorption likely occurs at specific sites on the cationic wood pulp with the PFASs adsorbing in one layer on the fiber surface.[46] Using the Langmuir model, we calculated that the maximum adsorption capacity (q_{max}) values for PFOS and PFOA were 763 and 605 mg/g, respectively. The difference in q_{max} between PFOS and PFOA is attributed to the sulfate group's increased affinity for electrostatic interactions with charged amine groups relative to the carboxylate.[47,48] Additionally, because PFASs are typically found at concentrations from single-digit ng/L to hundreds of μg/L in the environment,[5,6,49] we calculated distribution coefficients (K_D, L/g), which characterize the affinity of adsorbates for an adsorbent and estimate the magnitude of adsorption that will occur at low PFAS concentrations, using the isotherm data.[50−52] K_D values were determined using the linear portion of the adsorption isotherms (Figure S19) and resulted in log K_D values of 3.93 and 3.09 for PFOS and PFOA, respectively, which are comparable to other adsorbents.

Other PFAS Derivatives. In nature, water contains a mixture of different PFASs at low concentrations (i.e., single-digit ng/L to hundreds of μg/L).[5,6,49] To determine whether QWP1.5 was effective for removing multiple types of PFASs, we monitored PFAS adsorption after the cationic WP was mixed simultaneously with PFOS, PFOA, PFBS, PFBA, GenX, and 6:2 FTS (see Figure 4 for chemical structures). After just

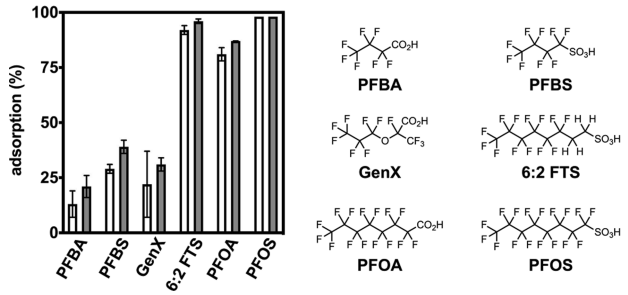

Figure 4. PFAS adsorption (%) on QWP1.5 with 30 s (white) and 60 min (gray) of contact time. ([QWP1.5] = 10.0 mg/L and $[PFAS]_0$ = ~2.5 μg/L.) Note: PFOS was removed below the limit of quantification (20 ng/L), so this limit was used in the adsorption % calculations.

30 s of contact time, we observed >80% adsorption of PFOS, PFOA, and 6:2 FTS (Figure 4). On the other hand, we found less efficient adsorption of PFBS, PFBA, and GenX, with adsorption between 13 and 29%. After 60 min of contact time, only small increases in PFAS adsorption were observed, with PFBS having the largest change from 29 to 39%. Combined, these data reveal the impact of PFAS chain length on adsorption because the PFASs with longer chain lengths (i.e., PFOS, PFOA, and 6:2 FTS) are adsorbed more efficiently than those with shorter chain lengths (i.e., PFBS and PFBA). To explain this phenomenon, we examined the PFASs' octanol/water partition coefficients (K_{ow}) that reflect a molecule's hydrophobicity. We found that longer PFASs had larger K_{ow}, meaning that they were more hydrophobic, likely due to their longer hydrophobic tails.[53,54] This finding suggests that hydrophobic interactions are likely complementing the electrostatic interactions during adsorption. More specifically, we propose that the cellulose's hydrophobic backbone is enhancing the QWP1.5's ability to efficiently adsorb the more hydrophobic (i.e., longer chain) PFASs. In addition, we observed that the PFAS functional group plays a role in adsorption, wherein the PFASs with sulfate groups were more effectively adsorbed than the PFASs with carboxyl groups. We again attribute the increased adsorption to the sulfate group's known increased affinity for electrostatic interactions with charged amine groups.[47,48] The adsorption trends found in this study are consistent with other reports in literature studies.[33,55,56]

Potential Interferents. Natural organic matter (NOM) refers to organic compounds naturally present in freshwater sources, and it has previously been shown to inhibit PFAS adsorption on conventional adsorbents.[57] To evaluate whether NOM inhibits adsorption with our cationic wood pulp fibers, we measured PFAS adsorption in the presence of humic acid (HA), a common type of NOM. We observed that HA significantly reduced PFAS adsorption, with ≤20% of each PFAS being adsorbed (Tables S16−S18). Because HA is a complex mixture of charged and uncharged species, and the hydrophobicity/hydrophilicity can vary based on the source, we measured the specific UV absorbance at 254 nm ($SUVA_{254}$) to characterize our HA (Figure S23).[58] The $SUVA_{254}$ was 4.1, which suggests that the HA mainly consists of high molecular weight hydrophobic and aromatic materials.[59] We hypothesize that HA is likely adsorbing to the wood pulp via hydrophobic interactions and blocking the PFAS access to the cationic sites. Further research is needed to attenuate the detrimental impact of NOM on these cationic WP-based adsorbents (e.g., by increasing the fluorophilicity[24]).

Water pH often adversely impacts PFAS adsorption because some adsorbents lose their cationic charge at environmentally relevant pHs of 5−9.[22,60] The QWPs synthesized herein, on the other hand, should not be impacted by pH because the quaternary amine has a pH-insensitive permanent charge. Moreover, the PFOS/PFOA studied herein have pK_a values below 3,[61,62] meaning that the sulfonyl and carboxyl groups will remain charged at pHs 5−9. As expected, after 30 s of contact time, we observed that pH had no effect on PFOS or PFOA adsorption (Figure 5a). Moreover, the leftover PFOS concentration in solution was below the limit of quantification (<20 ng/L), which is much lower than the EPA guidelines for PFOS in water.

The influence of salt concentration on PFAS adsorption was also studied because water tends to have low concentrations of

https://doi.org/10.1021/acsestwater.1c00396
ACS EST Water 2022, 2, 349−356

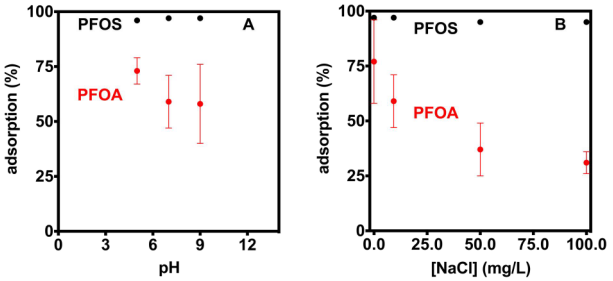

Figure 5. PFOS (black) and PFOA (red) adsorption (%) as a function of (A) pH and (B) NaCl concentration. ([QWP1.5] = 10.0 mg/L and $[PFAS]_{initial}$ < 2.8 μg/L.) Note: PFOS was removed below the limit of quantification (20 ng/L), so this limit was used for adsorption % calculations. Some error bars are not visible due to their small size.

inorganic ions.[19,20] After 30 s of contact time, we observed that the salt concentration had no impact on PFOS adsorption, similar to the pH experiment, with leftover PFOS concentrations below the limit of quantification (Figure 5b). In contrast, PFOA adsorption decreased from >75% to nearly 30% as the NaCl concentration increased from 0 to 100 mg/L, likely due to electrostatic shielding between PFOA and the wood pulp's cationic sites. The difference in PFOS and PFOA adsorption is attributed, again, to the increased sulfate affinity for cationic amines, as Schlenoff and co-workers showed that sulfate/amine interactions are less affected by NaCl concentrations than carboxylate/amine interactions.[48] Despite the reduction in PFOA adsorption, it remains high (>50%) for salt concentrations below 25 mg/L, which is the value usually observed in freshwater samples.[30,63]

Comparison with Other Adsorbents. To demonstrate that the rapid adsorption by QWP1.5 is advantageous compared to conventional adsorbents, we compared PFOS and PFOA adsorption at 30 s and 60 min of contact times with a commercial ion exchange resin (PFA 694E from Purolite) and granular AC (GAC, Filtrasorb 400) under environmentally relevant concentrations (~2.5 μg/L). As highlighted in Figure 6 (and Figure S22), QWP1.5 outperformed the other adsorbents at these short contact times. QWP1.5 was also found to be competitive with other sustainably sourced adsorbents based on the maximum PFOS/PFOA adsorption capacities (q_{max}) (see Table 1) and distribution coefficients (log K_D), which characterizes the affinity of adsorbates for an adsorbent.

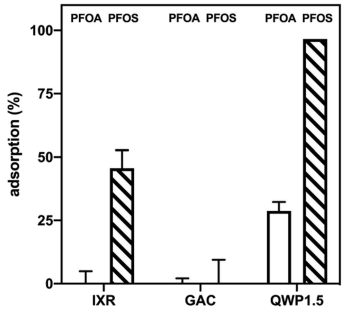

Figure 6. PFOS (striped) and PFOA (transparent) adsorption (%) as a function of the adsorbent after 30 s of contact time. ([adsorbent] = 10.0 mg/L and $[PFAS]_{initial}$ < 2.0 μg/L; IXR = Purolite PFA 694E and GAC = Filtrasorb 400.) Note: PFOS was removed below the limit of quantification (20 ng/L), so this limit was used for adsorption % calculations. Some error bars are not visible due to their small size.

Table 1. Comparison of Data with Other Adsorbents

material	PFAS	q_{max} (mg/g)	log K_D
QWP1.5	PFOS	763	3.93
	PFOA	605	3.09
GAC	both	<600[19]	<5[64]
anion exchange resins	both	200−2400[20]	~2−3[30]
PEI cellulose NCs	PFOA	2.32[33]	n.r.
functionalized cyclodextrins	PFOA	<500[65,66]	<4.0[30]
quaternary amine-funct. cotton	PFOS	1650[34]	n.r.
	PFOA	1284[34]	n.r.

A few shortcomings of QWP1.5 are the inefficient adsorption (<29%) of the shorter chain PFBS and PFBA and decreased adsorption of all PFAS (<20%) when humic acid was present. (Note that both GAC and anion-exchange resins are known to be similarly impacted by NOM).[31,55] Further modifications will be needed to attenuate the impact of HA on PFAS adsorption. To summarize, the main advantages of cationic WP are the competitive adsorption capacities and distribution coefficients as well as the rapid adsorption of long chain PFASs under environmentally relevant concentrations.

Degradation Versus Regeneration. While beyond the scope of this article, the fate of the spent QWP adsorbent eventually needs to be considered. Regeneration is often explored so that adsorbents can be reused; however, the processes involved in regeneration can potentially outweigh the benefits. For example, regenerating AC requires frequent costly and energy-intensive methods, while regenerating IX resins entails harsh solvent combinations that are not financially feasible for large-scale operations.[19,23,56,67] One potential advantage of these cellulose-based adsorbents is the potential for environmental biodegradation after PFAS removal via emerging technologies such as irradiation[68] or microbial digestion.[69]

CONCLUSIONS

In summary, we demonstrated herein that cationic wood pulp is a promising adsorbent for removing PFASs from water. Accessing QWP involves a straightforward, one-step reaction, wherein the resulting charge density can be tailored by varying the reactant concentrations. At environmentally relevant concentrations (~2.5 μg/L), PFOS and PFOA were adsorbed in under 30 s, making QWPs advantageous compared to other adsorbents that require long adsorption times (>15 min). The maximum adsorption capacity for PFOS and PFOA on QWP1.5 outperforms similar adsorbents and activated carbon. Although adsorption was impacted by natural organic matter, it was unaffected by solution pH and low salt concentrations. Further research is necessary to advance these materials, especially with respect to the competitive adsorption with hydrophobic organic matter. Nevertheless, these materials are promising because wood pulp is bio-sourced, biodegradable, and inexpensive (~$0.90 per metric ton in 2021).[70] For these reasons, we remain optimistic that functionalized wood pulp will become a competitive, renewable alternative adsorbent to activated carbon for PFAS removal.

https://doi.org/10.1021/acsestwater.1c00396
ACS EST Water 2022, 2, 349−356

■ ASSOCIATED CONTENT

Supporting Information

The Supporting Information is available free of charge at https://pubs.acs.org/doi/10.1021/acsestwater.1c00396.

Materials, general experimental procedures, QWP synthesis and characterization, PFAS adsorption experiments, and analytical methods (PDF)

■ AUTHOR INFORMATION

Corresponding Author

Anne J. McNeil − *Department of Chemistry and Macromolecular Science and Engineering Program, University of Michigan, Ann Arbor, Michigan 48109-1055, United States;* orcid.org/0000-0003-4591-3308; Email: ajmcneil@umich.edu

Authors

Justin T. Harris − *Department of Chemistry, University of Michigan, Ann Arbor, Michigan 48109-1055, United States;* orcid.org/0000-0002-6495-8248

Gloria D. de la Garza − *Department of Chemistry, University of Michigan, Ann Arbor, Michigan 48109-1055, United States;* orcid.org/0000-0003-4743-2698

Angela M. Devlin − *Department of Chemistry, University of Michigan, Ann Arbor, Michigan 48109-1055, United States*

Complete contact information is available at: https://pubs.acs.org/10.1021/acsestwater.1c00396

Author Contributions

J.T.H. was involved in conceptualization and methodology, as well as performed all syntheses, most characterization studies, and most adsorption experiments. In addition, J.T.H. was involved in formal analysis, visualization, and writing the original draft, as well as reviewing and editing final drafts. G.D.D. performed the adsorption experiments that compared our materials to commercial adsorbents, and created Figure 6. A.M.D. performed the Raman spectroscopic studies. Both G.D.D. and A.M.D. reviewed and edited final drafts. A.J.M. was involved in conceptualization, methodology, resources, supervision, funding acquisition, and writing the original and final drafts.

Notes

The authors declare no competing financial interest.

■ ACKNOWLEDGMENTS

This work was supported by the Department of Chemistry at the University of Michigan. G.D.D. thanks the National Science Foundation for a Graduate Research Fellowship. The Raman spectroscopy was supported by a Department of Energy (DE-SC0004888) grant to Prof. Adam Matzger. We thank Cellulose Lab for generously providing wood pulp, Tom Yavarski for analyzing HA samples, Zhongrui (Jerry) Li for SEM/Auger analysis, and Dr. Yongtao Li from Eurofins Eaton Analytical for generously donating PFAS-free water and tubes, as well as helpful discussions regarding PFAS analysis.

■ REFERENCES

(1) Boretti, A.; Rosa, L. Reassessing the projections of the world water development report. *npj Clean Water* **2019**, *2*, 15.

(2) Hu, X. C.; Andrews, D. Q.; Lindstrom, A. B.; Bruton, T. A.; Schaider, L. A.; Grandjean, P.; Lohmann, R.; Carignan, C. C.; Blum, A.; Balan, S. A.; Higgins, C. P.; Sunderland, E. M. Detection of poly- and perfluoroalkyl substances (PFASs) in U.S. drinking water linked to industrial sites, military fire training areas, and wastewater treatment plants. *Environ. Sci. Technol. Lett.* **2016**, *3*, 344−350.

(3) Bai, X.; Son, Y. Perfluoroalkyl substances (PFAS) in surface water and sediments from two urban watersheds in Nevada, USA. *Sci. Total Environ.* **2021**, *751*, 141622.

(4) Barton, K. E.; Starling, A. P.; Higgins, C. P.; McDonough, C. A.; Calafat, A. M.; Adgate, J. L. Sociodemographic and behavioral determinants of serum concentrations of per- and polyfluoroalkyl substances in a community highly exposed to aqueous film-forming foam contaminants in drinking water. *Int. J. Hyg. Environ. Health* **2020**, *223*, 256−266.

(5) Boone, J. S.; Vigo, C.; Boone, T.; Byrne, C.; Ferrario, J.; Benson, R.; Donohue, J.; Simmons, J. E.; Kolpin, D. W.; Furlong, E. T.; Glassmeyer, S. T. Per- and polyfluoroalkyl substances in source and treated drinking waters of the United States. *Sci. Total Environ.* **2019**, *653*, 359−369.

(6) Nickerson, A.; Rodowa, A. E.; Adamson, D. T.; Field, J. A.; Kulkarni, P. R.; Kornuc, J. J.; Higgins, C. P. Spatial trends of anionic, zwitterionic, and cationic PFASs at an AFFF-impacted site. *Environ. Sci. Technol.* **2021**, *55*, 313−323.

(7) Barzen-Hanson, K. A.; Roberts, S. C.; Choyke, S.; Oetjen, K.; McAlees, A.; Riddell, N.; McCrindle, R.; Ferguson, P. L.; Higgins, C. P.; Field, J. A. Discovery of 40 classes of per- and polyfluoroalkyl substances in historical aqueous film-forming foams (AFFFs) and AFFF-impacted groundwater. *Environ. Sci. Technol.* **2017**, *51*, 2047−2057.

(8) Kissa, E. *Fluorinated surfactants and repellants*; 2nd Edition, Marcell Dekker, Inc. 2001.

(9) Kotthoff, M.; Muller, J.; Jurling, H.; Schlummer, M.; Fiedler, D. Perfluoroalkyl and polyfluoroalkyl substances in consumer products. *Environ. Sci. Pollut. Res.* **2015**, *22*, 14546−14559.

(10) U.S. EPA. *PFOA Stewardship Program Baseline Year Summary Report*. https://www.epa.gov/assessing-and-managing-chemicals-under-tsca/pfoa-stewardship-program-baseline-year-summary-report (accessed March 11, 2021).

(11) Stahl, T.; Mattern, D.; Brunn, H. Toxicology of perfluorinated compounds. *Environ. Sci. Eur.* **2011**, *23*, 38.

(12) Chohan, A.; Petaway, H.; Rivera-Diaz, V.; Day, A.; Colaianni, O.; Keramati, M. Per and polyfluoroalkyl substances scientific literature review: water exposure, impact on human health, and implications for regulatory reform. *Rev. Environ. Health* 2021, DOI: 10.1515/reveh-2020-0049.

(13) Cordner, A.; De La Rosa, V. Y.; Schaider, L. A.; Rudel, R. A.; Richter, L.; Brown, P. Guideline levels for PFOA and PFOS in drinking water: the role of scientific uncertainty, risk assessment decisions, and social factors. *J. Exposure Sci. Environ. Epidemiol.* **2019**, *29*, 157−171.

(14) Interstate Technology and Regulatory Council (ITRC). *ITRC PFAS regulations, guidance and advisories fact sheets*. https://pfas-1.itrcweb.org/fact-sheets/ (accessed March 11, 2021).

(15) *Fact sheet: PFOA and PFOS drinking water health advisories*; EPA 800-F-16-003; U.S. EPA: Washington, DC, 2016.

(16) Michigan Department of Environment, Great Lakes, and Energy. *New state drinking water standards pave way for expansion of Michigan's PFAS clean-up efforts*. https://www.michigan.gov/egle/0,9429,7-135--535602--,00.html (accessed March 11, 2021).

(17) EWG. *Mapping the PFAS contamination crisis: new data show 2,337 sites in 49 States*. https://www.ewg.org/interactive-maps/pfas_contamination/ (accessed March 11, 2021).

(18) Kucharzyk, K. H.; Darlington, R.; Benotti, M.; Deeb, R.; Hawley, E. Novel treatment technologies for PFAS compounds: A critical review. *J. Environ. Manage.* **2017**, *204*, 757−764.

(19) Du, Z.; Deng, S.; Bei, Y.; Huang, Q.; Wang, B.; Huang, J.; Yu, G. Adsorption behavior and mechanism of perfluorinated compounds on various adsorbents—A review. *J. Hazard. Mater.* **2014**, *274*, 443−454.

(20) Zhang, D. Q.; Zhang, W. L.; Liang, Y. N. Adsorption of perfluoroalkyl and polyfluoroalkyl substances (PFASs) from aqueous solution - A review. *Sci. Total Environ.* **2019**, *694*, 133606.
(21) Xiao, X.; Ulrich, B. A.; Chen, B.; Higgins, C. P. Sorption of poly- and perfluoroalkyl substances (PFASs) relevant to aqueous film-forming foam (AFFF)-impacted groundwater by biochars and activated carbon. *Environ. Sci. Technol.* **2017**, *51*, 6342−6351.
(22) Yu, Q.; Zhang, R.; Deng, S.; Huang, J.; Yu, G. Sorption of perfluorooctane sulfonate and perfluorooctanoate on activated carbons and resin: kinetic and isotherm study. *Water Res.* **2009**, *43*, 1150−1158.
(23) Zaggia, A.; Conte, L.; Falletti, L.; Fant, M.; Chiorboli, A. Use of strong anion exchange resins for the removal of perfluoroalkylated substances from contaminated drinking water in batch and continuous pilot plants. *Water Res.* **2016**, *91*, 137−146.
(24) Kumarasamy, E.; Manning, I. M.; Collins, L. B.; Coronell, O.; Leibfarth, F. A. Ionic fluorogels for remediation of per- and polyfluorinated alkyl substances from water. *ACS Cent. Sci.* **2020**, *6*, 487−492.
(25) Ateia, M.; Arifuzzaman, M.; Pellizzeri, S.; Attia, M. F.; Tharayil, N.; Anker, J. N.; Karanfil, T. Cationic polymer for selective removal of GenX and short-chain PFAS from surface waters and wastewaters at ng/L levels. *Water Res.* **2019**, *163*, 114874.
(26) Alsbaiee, A.; Smith, B. J.; Xiao, L.; Ling, Y.; Helbling, D.; Dichtel, W. Rapid removal of organic micropollutants from water by a porous β-cyclodextrin polymer. *Nature* **2016**, *529*, 190−194.
(27) Ling, Y.; Klemes, M. J.; Xiao, L.; Alsbaiee, A.; Dichtel, W. R.; Helbling, D. E. Benchmarking micropollutant removal by activated carbon and porous β-cyclodextrin polymers under environmentally relevant scenarios. *Environ. Sci. Technol.* **2017**, *51*, 7590−7598.
(28) Klemes, M. J.; Ling, Y.; Ching, C.; Wu, C.; Xiao, L.; Helbling, D. E.; Dichtel, W. R. Reduction of a tetrafluoroterephthalonitrile-β-cyclodextrin polymer to remove anionic micropollutants and perfluorinated alkyl substances from water. *Angew. Chem., Int. Ed.* **2019**, *58*, 12049−12053.
(29) Wu, C.; Klemes, M. J.; Trang, B.; Dichtel, W. R.; Helbling, D. E. Exploring the factors that influence the adsorption of anionic PFAS on conventional and emerging adsorbents in aquatic matrices. *Water Res.* **2020**, *182*, 115950.
(30) Ching, C.; Klemes, M. J.; Trang, B.; Dichtel, W. R.; Helbling, D. E. β-cyclodextrin polymers with different cross-linkers and ion-exchange resins exhibit variable adsorption of anionic, zwitterionic, and nonionic PFASs. *Environ. Sci. Technol.* **2020**, *54*, 12693−12702.
(31) Wang, R.; Ching, C.; Dichtel, W. R.; Helbling, D. E. Evaluating the removal of per- and polyfluoroalkyl substances from contaminated groundwater with different adsorbents using a suspect screening approach. *Environ. Sci. Technol. Lett.* **2020**, *7*, 954−960.
(32) Hokkanen, S.; Bhatnagar, A.; Sillanpaa, M. A review on modification methods to cellulose-based adsorbents to improve adsorption capacity. *Water Res.* **2016**, *91*, 156−173.
(33) Ateia, M.; Attia, M. F.; Maroli, A.; Tharayil, N.; Alexis, F.; Whitehead, D. C.; Karanfil, T. Rapid removal of poly- and perfluorinated alkyl substances by poly(ethylenimine)-functionalized cellulose microcrystals at environmentally relevant conditions. *Environ. Sci. Technol. Lett.* **2018**, *5*, 764−769.
(34) Deng, S.; Zheng, Y. Q.; Xu, F. J.; Wang, B.; Huang, J.; Yu, G. Highly efficient sorption of perfluorooctane sulfonate and perfluorooctanoate on a quaternized cotton prepared by atom transfer radical polymerization. *Chem. Eng. J.* **2012**, *193*−*194*, 154−160.
(35) Harris, J. T.; McNeil, A. J. Localized hydrogels based on cellulose nanofibers and wood pulp for rapid removal of methylene blue. *J. Polym. Sci.* **2020**, *58*, 3042−3049.
(36) *Biermann's Handbook of Pulp and Paper;* 3rd ed.; Bajpai, P., Ed.; Elsevier, 2018.
(37) Olszewska, A.; Eronen, P.; Johansson, L.; Malho, J.; Ankerfors, M.; Lindstrom, T.; Ruokolainen, J.; Laine, J.; Osterberg, M. The behaviour of cationic nanofibrillar cellulose in aqueous media. *Cellulose* **2011**, *18*, 1213−1226.
(38) Odabas, N.; Amer, H.; Bacher, M.; Henniges, U.; Potthast, A.; Rosenau, T. Properties of cellulosic material after cationization in different solvents. *ACS Sustainable Chem. Eng.* **2016**, *4*, 2295−2301.
(39) Wang, Z.; Carlsson, D.; Tammela, P.; Hua, K.; Zhang, P.; Nyholm, L.; Stromme, M. Surface modified nanocellulose fibers yield conducting polymer-based flexible supercapacitors with enhanced capacitances. *ACS Nano* **2015**, *9*, 7563−7571.
(40) de la Motte, H.; Westman, G. Regioselective cationization of cellulosic materials using an efficient solvent-minimizing spray-technique. *Cellulose* **2012**, *19*, 1677−1688.
(41) Loubaki, E.; Ourevitch, M.; Sicsic, S. Chemical modification of chitosan by glycidyl trimethylammonium chloride. Characterization of modified chitosan by ^{13}C and ^{1}H NMR spectroscopy. *Eur. Polym. J.* **1991**, *27*, 311−317.
(42) Golizadeh, M.; Karimi, A.; Gandomi-Ravandi, S.; Vossoughi, M.; Khafaji, M.; Joghataei, M. T.; Faghihi, F. Evaluation of cellular attachment and proliferation on different surface charged functional cellulose electrospun nanofibers. *Carbohydr. Polym.* **2019**, *207*, 796−805.
(43) Agarwal, U. P.; Ralph, S. A.; Reiner, R. S.; Baez, C. Probing crystallinity of never-dried wood cellulose with Raman spectroscopy. *Cellulose* **2016**, *23*, 125−144.
(44) Wikberg, H.; Maunu, S. L. Characterisation of thermally modified hard- and softwoods by ^{13}C CPMAS NMR. *Carbohydr. Polym.* **2004**, *58*, 461−466.
(45) Pigorsch, E. Spectroscopic characterisation of cationic quaternary ammonium starches. *Starch* **2009**, *61*, 129−138.
(46) Limousin, G.; Gaudet, J.-P.; Charlet, L.; Szenknect, S.; Barthes, V.; Krimissa, M. Sorption isotherms: A review on physical bases, modeling and measurement. *Appl. Geochem.* **2007**, *22*, 249−275.
(47) Dubas, S. T.; Schlenoff, J. B. Swelling and smoothing of polyelectrolyte multilayers by salt. *Langmuir* **2001**, *17*, 7725−7727.
(48) Fu, J.; Fares, H. M.; Schlenoff, J. B. Ion-pairing strength in polyelectrolyte complexes. *Macromolecules* **2017**, *50*, 1066−1074.
(49) Crone, B. C.; Speth, T. F.; Wahman, D. G.; Smith, S. J.; Abulikemu, G.; Kleiner, E. J.; Pressman, J. G. Occurrence of per- and polyfluoroalkyl substances (PFAS) in source water and their treatment in drinking water. *Crit. Rev. Environ. Sci. Technol.* **2019**, *49*, 2359−2396.
(50) Kamlet, M. J.; Doherty, R. M.; Abraham, M. H.; Taft, R. W. Linear solvation energy relationships. 33. An analysis of the factors that influence adsorption of organic compounds on activated carbon. *Carbon* **1985**, *23*, 549−554.
(51) Luehrs, D. C.; Hickey, J. P.; Nilsen, P. E.; Godbole, K. A.; Rogers, T. N. Linear solvation energy relationship of the limiting partition coefficient of organic solutes between water and activated carbon. *Environ. Sci. Technol.* **1996**, *30*, 143−152.
(52) Ling, Y.; Klemes, M. J.; Steinschneider, S.; Dichtel, W. R.; Helbling, D. E. QSARs to predict adsorption affinity of organic micropollutants for activated carbon and β-cyclodextrin polymer adsorbents. *Water Res.* **2019**, *154*, 217−226.
(53) Deng, S.; Zhang, Q.; Nie, Y.; Wei, H.; Wang, B.; Huang, J.; Yu, G.; Xing, B. Sorption mechanisms of perfluorinated compounds on carbon nanotubes. *Environ. Pollut.* **2012**, *168*, 138−144.
(54) Arp, H. P. H.; Niederer, C.; Goss, K.-U. Predicting the partitioning behavior of various highly fluorinated compounds. *Environ. Sci. Technol.* **2006**, *40*, 7298−7304.
(55) Gagliano, E.; Sgroi, M.; Falciglia, P. P.; Vagliasindi, F. G. A.; Roccaro, P. Removal of poly- and perfluoroalkyl substances (PFAS) from water by adsorption: Role of PFAS chain length, effect of organic matter and challenges in adsorbent regeneration. *Water Res.* **2020**, *171*, 115381.
(56) Eschauzier, C.; Beerendonk, E.; Scholte-Veenendaal, P.; De Voogt, P. Impact of treatment processes on the removal of perfluoroalkyl acids from the drinking water production chain. *Environ. Sci. Technol.* **2012**, *46*, 1708−1715.
(57) Yu, J.; Lv, L.; Lan, P.; Zhang, S.; Pan, B.; Zhang, W. Effect of effluent organic matter on the adsorption of perfluorinated

https://doi.org/10.1021/acsestwater.1c00396
ACS EST Water 2022, 2, 349−356

compounds onto activated carbon. *J. Hazard. Mater.* **2012**, *225*, 99−106.
(58) Sillanpää, M.; Matilainen, A.; Lahtinen, T. Characterization of NOM. In *Natural Organic Matter in Water*; 1st edition; IWA Publishing, 2015, pp. 17−53.
(59) Edzwald, J. K.; Tobiason, J. E. Enhanced coagulation: US requirements and a broader view. *Water Sci. Technol.* **1999**, *40*, 63−70.
(60) Dixit, F.; Barbeau, B.; Mostafavi, S. G.; Mohseni, M. PFOA and PFOS removal by ion exchange for water reuse and drinking applications: role of organic matter characteristics. *Environ. Sci.: Water Res. Technol.* **2019**, *5*, 1782−1795.
(61) Goss, K.-U. The pKa values of PFOA and other highly fluorinated carboxylic acids. *Environ. Sci. Technol.* **2008**, *42*, 456−458.
(62) Brooke, D.; Footitt, A.; Nwaogu, T. A. *Environmental Risk Evaluation Report: Perfluorooctanesulphonate (PFOS)*; Environment Agency, 2004.
(63) Ling, Y.; Alzate-Sanchez, D. M.; Klemes, M. J.; Dichtel, W. R.; Helbling, D. E. Evaluating the effects of water matrix constituents on micropollutant removal by activated carbon and β-cyclodextrin polymer adsorbents. *Water Res.* **2020**, *173*, 115551.
(64) Liu, C. J.; Werner, D.; Bellona, C. Removal of per- and polyfluoroalkyl substances (PFASs) from contaminated groundwater using granular activated carbon: a pilot-scale study with breakthrough modeling. *Environ. Sci.: Water Res. Technol.* **2019**, *5*, 1844−1853.
(65) Yang, A.; Ching, C.; Easler, M.; Helbling, D. E.; Dichtel, W. R. Cyclodextrin polymers with nitrogen-containing tripodal crosslinkers for efficient PFAS adsorption. *ACS Materials Lett.* **2020**, *2*, 1240−1245.
(66) Xiao, L.; Ling, Y.; Alsbaiee, A.; Li, C.; Helbling, D. E.; Dichtel, W. R. β-cyclodextrin polymer network sequesters perfluorooctanoic acid at environmentally relevant concentrations. *J. Am. Chem. Soc.* **2017**, *139*, 7689−7692.
(67) San Miguel, G.; Lambert, S. D.; Graham, N. J. D. The regeneration of field-spent granular activated carbons. *Water Res.* **2001**, *35*, 2740−2748.
(68) Trojanowicz, M.; Bartosiewicz, I.; Bojanowska-Czajka, A.; Szreder, T.; Bobrowski, K.; Nalecz-Jawecki, G.; Meczynska-Wielgosz, S.; Nichipor, H. Application of ionizing radiation in decomposition of perfluorooctane sulfonate (PFOS) in aqueous solutions. *Chem. Eng. J.* **2020**, *379*, 122303.
(69) Huang, S.; Jaffe, P. R. Defluorination of perfluorooctanoic acid (PFOA) and perfluorooctane sulfonate (PFOS) by Acidimicrobium sp. Strain A6. *Environ. Sci. Technol.* **2019**, *53*, 11410−11419.
(70) index mundi. *Wood Pulp Monthly Price*.https://www.indexmundi.com/commodities/?commodity=wood-pulp&months=120&currency=eur (accessed April 16, 2021).

https://doi.org/10.1021/acsestwater.1c00396
ACS EST Water 2022, 2, 349−356